



HAL
open science

MRI-free neuronavigation for transcranial magnetic stimulation in severe depression

Benoît Combès, Charles Garraud, Xavier Morandi, Sylvain Prima, Pierre Hellier

► **To cite this version:**

Benoît Combès, Charles Garraud, Xavier Morandi, Sylvain Prima, Pierre Hellier. MRI-free neuronavigation for transcranial magnetic stimulation in severe depression. MICCAI Workshop on Mesh Processing in Medical Image Analysis (MeshMed'2011), Sep 2011, Canada. pp.29-38. inserm-00633573

HAL Id: inserm-00633573

<https://inserm.hal.science/inserm-00633573>

Submitted on 18 Oct 2011

HAL is a multi-disciplinary open access archive for the deposit and dissemination of scientific research documents, whether they are published or not. The documents may come from teaching and research institutions in France or abroad, or from public or private research centers.

L'archive ouverte pluridisciplinaire **HAL**, est destinée au dépôt et à la diffusion de documents scientifiques de niveau recherche, publiés ou non, émanant des établissements d'enseignement et de recherche français ou étrangers, des laboratoires publics ou privés.

MRI-free neuronavigation for transcranial magnetic stimulation in severe depression

Benoît Combès^{a,b,c}, Charles Garraud^{a,e}, Xavier Morandi^{a,b,c,d}, Sylvain Prima^{a,b} and Pierre Hellier^{a,e}

^aINRIA, VisAGeS Project-Team, F-35042 Rennes, France

^bINSERM, U746, F-35042 Rennes, France

^cUniversity of Rennes I, F-35043 Rennes, France

^dPontchaillou Univ. Hospital, Department of Neurosurgery, F-35033 Rennes, France

^eSyneika, F-35000 Rennes, France

Abstract. This paper presents a MRI-free neuronavigation technique for repetitive transcranial magnetic stimulation (rTMS). This method is composed of three steps: 1) surface sampling of the subject’s scalp and face thanks to a 3D tracker, followed by Poisson surface reconstruction, 2) non-linear surface registration of an atlas surface to the extracted surface using an efficient modified non-linear EM-ICP algorithm [2], and 3) extrapolation of the transformation to a cortical stimulation target. Results have been obtained on a database of 10 subjects and have shown an accuracy of 10.2 mm. Although clearly less accurate than neuronavigation on the subject’s MRI, we advocate that this neuronavigation method is reproducible and acceptable for routine application of rTMS in severe depression.

1 Introduction

Repetitive transcranial magnetic stimulation (rTMS) is a cortical stimulation technique where a strong electromagnetic field is generated by a coil. The field modifies the neuronal activity beneath the coil and since the stimulation is focal, rTMS has a broad range of potential applications in psychiatry and neurology [13]. It has been recently shown that there is some correlation between the stimulation accuracy and the therapeutic efficacy [4]. Therefore, the stimulation is preferably conducted using a neuronavigation system [11] that allows one to visualize the actual stimulation locus on the subject’s MRI; thus the clinician can move the coil so that the stimulation is at the planned anatomical target defined on the MRI prior to stimulation. In this paper, we propose a new method that allows neuronavigation without MRI in the context of rTMS for severe, drug-resistant depression. It is generally admitted that a good stimulation target for depression is the dorsolateral prefrontal cortex (DLPFC), defined as Brodmann areas 9-46 in [12]. There is a huge number of patients with severe depression that could benefit from rTMS but the cost of the MRI scan, together with the waiting time (approximately between 5 and 15 weeks depending on countries), is a bottleneck for widespread MRI-based neuronavigated rTMS. We

argue that a system that would allow a fast, MRI-free navigation with a slightly degraded accuracy but an excellent reproducibility between sessions would be valuable in clinical routine. Hence, in this paper we propose a surface-based neuronavigation on atlas for rTMS. Firstly, the subject’s skin surface (scalp and face) is sampled thanks to a pointer localized by a 3D tracker of the neuronavigation system and reconstructed using the Poisson method. Secondly, the atlas surface, on which the stimulation target has been localized beforehand, is registered to the subject’s surface thanks to an EM-ICP non-linear registration technique. Thirdly, the non-linear transformation computed on the surface is extrapolated to the cortical stimulation target to predict the patient’s stimulation target for treatment-resistant depression. Accuracy was evaluated on a dataset of 10 subjects and was found to be 10.2 mm on average. The closest work to our method was presented in [8], where the authors used a small number of surface points (22) to register a database of 56 subjects so as to create a functional probabilistic atlas. In our paper, the atlas is deformed toward the subject using a large number of points (generally, several thousands) and an anatomical target is transformed and used in the neuronavigation system to guide a rTMS coil.

2 Material and method

2.1 Method overview

An overview of the method is presented in Figure 1. For a given subject, a surface sampling is first performed, using a pointer tracked by a 3D localizer of the neuronavigation system. Then, the segmented surface of the atlas X is registered to the subject’s surface Y and the resulting transformation T is used to map the coordinates of the target into the subject’s space. The data are then used by the neuronavigation system to guide the rTMS coil. The next sections will describe the following steps: surface acquisition and reconstruction of Y in Section 2.2 and surface registration of X to Y in Section 2.3. Visual results are presented in Section 3.

2.2 Surface acquisition and reconstruction

Anatomical sampling of the subject’s scalp and face is performed using an optical tracking system (Claron Technology Inc., Toronto) composed of the Micron-Tracker camera and recognized markers. Sampling of points is achieved by covering the subject’s head with the calibrated pointer tooltip. A software module was developed to record 4 anatomical landmarks denoted as L^Y on the subject’s head (inion, nasion, left and right tragus) used for an initial landmark-based registration (coined the LDM method hereafter) and then at least 100 surface points. The average number of samples was 3500 points, and the maximal sampling time was 10 minutes.

Then, the set of unorganized points is processed and a closed surface is reconstructed: firstly, the point set is processed through functions dedicated to

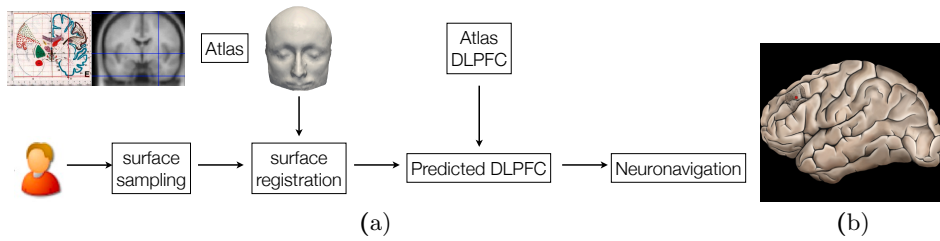


Fig. 1. (a): overview of the surface-based neuronavigation on atlas. (b): a surface rendering of the cortex with the Brodmann area 9/46, or DLPFC, dashed on the surface. To compute Euclidean errors, the area is identified as the centroid, represented here as the red point.

smoothing, outliers removal, normal estimation using the CGAL library [6]. The output is an oriented, smoothed point set suitable for surface reconstruction. Secondly, a surface reconstruction algorithm is applied to generate an iso-surface from the oriented pre-processed point set. 3D surface reconstruction from points set is a well-studied issue. Commonly used surface reconstruction techniques are based on Delaunay triangulation, implicit functions or parametric models. Given that the output of the pre-processing stage is a non-uniform, outlier reduced and smoothed point set, the reconstruction method used in our study should (1) infer the topology of the unknown surface, (2) fit the data, and (3) fill holes. For these reasons, the Poisson reconstruction technique is used [7]. This method allows reconstruction with greater details than other techniques. An implementation of the Poisson surface reconstruction algorithm based on the VTK framework [3] was used. This process produces the point set Y describing the subject's scalp and face, along with the landmark set L^Y .

2.3 Surface registration: efficient EM-ICP algorithm for linear and non-linear registration

In this section, we show how to compute the transformation T that best superposes the surface of the atlas X on the surface of the subject Y (using additional landmarks $L^X = (l_k^X)$ and $L^Y = (l_k^Y)$) so as to compute the coordinates of the target in the subject's space.

General scheme The EM-ICP algorithm [5] is an efficient and elegant solution for rigid registration of point sets. It relies on a probabilistic modeling of the point-to-point correspondences that allows i) a pragmatic definition of the superimposition of two point sets and ii) to deal with a relatively smooth cost function to minimize (in contrast to the classical ICP algorithm). Moreover, it is mathematically well-grounded (monotonic convergence), generic (no assumption on tessellation/topology/number of points) and can be specialized in many ways (*e.g.* to deal with non-linear deformations or to estimate shape models [1]).

Most importantly, the EM-ICP algorithm [5] allows dealing very efficiently and robustly with large point sets. This algorithm can be shown to be equivalent to the alternated iterative minimization of an energetic criterion. In this work, we propose a slight modification of the underlying criterion that allows one i) to use pairs of landmarks to constrain the registration, ii) to symmetrize the estimation of point-to-point correspondences and iii) to add a regularization on T to deal with non-linear deformations:

$$\begin{aligned} \mathcal{E}(T(X), Y, A, B) = & \sum_{j,k} (A_{jk} + B_{jk}) \rho_{\delta}(\|y_j - T(x_k)\|^2) + 2\sigma^2 \beta \sum_k \|l_k^Y - T(l_k^X)\|^2 \\ & + 2\sigma^2 \sum_{j,k} A_{jk} \log(A_{jk}) + 2\sigma^2 \sum_{j,k} B_{jk} \log(B_{jk}) + 2\sigma^2 \alpha L(T), \end{aligned}$$

with $\forall j, \sum_k A_{jk} = 1$ and $\forall k, \sum_j B_{jk} = 1$ (1)

where

- if we drop matrix B for a moment, for the sake of clarity, $A = (A_{jk})$ is the unknown *match* matrix encoding the *a posteriori* probabilities of correspondence between points of X and Y . This probabilistic interpretation of A is made possible thanks to the barrier function $\sum_{j,k} A_{jk} \log(A_{jk})$ [1]. In essence, the greater A_{jk} , the more likely the point $x_k \in X$ to be the correspondent of the point $y_j \in Y$. σ^2 is the Gaussian noise variance of X . This fuzzy control on the correspondences allows one to handle problems due to differences of sampling/number of points between X and Y : we do not look for one-to-one correspondences between points of each surface but instead for “fuzzy” correspondences linking each point of Y to each point of X . This match matrix is a row stochastic matrix, which leads to many-to-one correspondences. This asymmetric formulation makes the algorithm unable to achieve a good matching in specific cases and can make the choice of the source and target sets critical. To tackle this problem, our criterion also contains a second match matrix B , that is column stochastic, in addition to the row stochastic matrix A . The *a posteriori* probabilities of correspondences between points of X and Y is encoded in both matrices A and B , making the point-to-point matching much more symmetrical compared to [5].
- T is a transformation (to be later defined) superposing X on Y . This transformation is subject to a regularizer L .
- α and β are two positive parameters weighing respectively the regularization $L(T)$ term and the landmark-to-landmark discrepancy term $\sum_k \|l_k^Y - T(l_k^X)\|^2$ over the other terms.

- the function $(\rho_\delta : r \mapsto r \text{ if } r < \delta \text{ and } \delta \text{ else})$ is a robust function allowing points of X (resp. Y) having no homologue in Y (resp. X) to be discarded from the estimation of T .

It can be shown that the criterion \mathcal{E} can be minimized over the three unknown parameters T , A and B using the following two-step algorithm:

Algo NL-Sym-EM-ICP: Symmetric robust non-linear EM-ICP with landmarks

Step 1:

initialise \tilde{A} and \tilde{B} to the null matrix

$\forall x_k \in X;$

$\mathcal{S} = \{y_j \in Y \text{ such that } \|y_j - \tilde{T}(x_k)\|^2 < \delta\}$ (using a *kd-tree*)

$\forall y_j \in \mathcal{S};$

$\forall y_j \in \mathcal{S}; \tilde{A}_{jk} = \exp(-(\|y_j - \tilde{T}(x_k)\|^2 / (2\sigma^2)))$

$\forall y_j \notin \mathcal{S}; \tilde{A}_{jk}$ is left equal to 0

$\tilde{B} = \tilde{A}$

normalise \tilde{A} in rows and \tilde{B} in columns

compute the vectors $(\tilde{p}_j) : \forall j, \tilde{p}_j = 0$ if $\sum_i \tilde{A}_{ji} = 0$ and 1 else

compute the vectors $(\tilde{q}_k) : \forall k, \tilde{q}_k = 0$ if $\sum_i \tilde{B}_{ik} = 0$ and 1 else

Step 2: solve the approximation problem:

$\arg \min_T \sum_{j,k} (\tilde{p}_j \tilde{A}_{jk} + \tilde{q}_k \tilde{B}_{jk}) \|y_j - T(x_k)\|^2 + 2\sigma^2 \beta \sum_k \|T(l_k^X) - l_k^Y\|^2 + 2\sigma^2 \alpha L(T)$

Specifying T/L In practice, we design a coarse-to-fine approach to estimate T by first computing the rigid transformation best superposing L^X on L^Y and then using the NL-Sym-EM-ICP algorithm by modeling T successively as a rigid R , an affine F and a non-linear transformation W . For rigid and affine transformations T , we take $L(T) = 0$ and Step 2 has a closed-form solution. For the non-linear transformation, we parametrize W as a deformation field (*i.e.* $W(x) = x + t(x)$) and design L as a scalar Fourier-based regularizer over t :

$$L(t = (t_1, t_2, t_3)^T) = L(t_1) + L(t_2) + L(t_3), \text{ with } L(t_i) = \frac{1}{(2\pi)^3} \int_{-\infty}^{\infty} \frac{|t_i^*(\omega)|^2}{\phi^*(|\omega|/b)} d\omega,$$

where $*$ is the Fourier transform operator, $\phi : \mathbb{R} \rightarrow \mathbb{R}$ is an integrable function and b is a real strictly positive rescaling factor. We choose ϕ as a Wu compactly supported positive definite kernel. The advantage of such a regularization (over the TPS regularizer for example) is that it i) provides efficient solutions for Step 2 based on sparse linear algebra [14] and ii) introduces a scaling parameter b . The larger the b value, the more drastic the penalization of the high frequencies, *i.e.* by choosing a large b value, we focus on capturing the global/high-scale deformation superposing X and Y .

Interpolating the target position Each estimated transformation R , F and W is defined over \mathbb{R}^3 and has a closed-form expression. As a result, any point y of Y (thus those representing the DLPFC) can be mapped in the space of X as $y' = W(F(R(y)))$.

2.4 Material

Phantom To assess the accuracy of the point acquisition and reconstruction steps, a human-head phantom was used, shown in Figure 2-(a). The phantom was scanned with an isotropic 0.5 mm resolution CT (size $512 \times 512 \times 841$). A set of 4099 points was acquired as described in Section 2.2. The surface of the phantom was extracted using heuristic thresholding and mathematical morphology operators.

Subjects The experiments were performed using anatomical brain MRI of 10 healthy volunteers. Each subject had a brain MRI scan using a 3D T1-weighted sequence with 1 mm isotropic resolution, and the skin surface was extracted using thresholding and mathematical morphology operators. On the subjects, the surface representing the scalp and face was sampled using the process described in Section 2.2.

MRI Atlas In the experiments, the MRI atlas described in [9] was used. The skin surface was extracted using thresholding and mathematical morphology operators, and the four landmark points L^X were manually localized. This atlas was used instead of the Colin27 atlas since on the latter, the surface extraction process is difficult due to an antenna visible on the top of the atlas.

DLPFC localization Manual positioning of the DLPFC on the subjects' MRI and on the atlas was performed by an expert in neuroanatomy. The DLPFC was defined as the second third, *i.e.* middle part, of the middle frontal gyrus along the antero-posterior axis, corresponding to Brodmann areas 9/46 as described in [12], and as shown in Figure 1-(b). We have chosen to characterize the position of the DLPFC by its centroid, shown by the red dot. Therefore, hereafter the DLPFC is considered as a point, what enables to compute Euclidean distances between estimated targets and reference targets.

3 Validation and results

3.1 Poisson reconstruction accuracy

The point set acquired on the physical phantom was registered to the phantom's skin surface extracted from the CT using a rigid EM-ICP. The computed transformation was then applied to the reconstructed Poisson surface. The mean point-to-point error between the Poisson surface and the surface extracted from

the CT scan was 1.6 mm (standard deviation 1.08 mm). Results are presented in Figure 2. These results demonstrate the accuracy of the point sampling and show that the reconstructed surface is valid to represent the subject’s scalp and face.

3.2 Distance between predicted and reference DLPFC

The skin surface extracted on the MRI was registered toward the Poisson reconstructed surface using rigid EM-ICP. On the other side, the Poisson reconstructed surface was registered toward the atlas skin surface using the non-linear EM-ICP. Therefore, the predicted DLPFC can be compared to the reference DLPFC. Various degrees of freedom of the transformation were tested: landmark-based registration that corresponds to a Procrustes alignment using the 4 anatomical landmarks (LDM), LDM followed by a rigid registration (R), R followed by an affine registration (RA) and RA followed by a non-linear registration (NL). Table 1 shows the obtained errors for the 10 subjects for all transformations. Firstly, it can be observed that the mean error decreases when the degrees of freedom of the transformation increase. Secondly, the error obtained with the fully non-linear method is 10.2 mm on average. These results are discussed hereafter.

4 Conclusion

In this paper, a new method was proposed to perform neuronavigation without MRI for transcranial magnetic stimulation. The method is based on a subject’s surface sampling and reconstruction, followed by a non-linear registration of an atlas surface to the obtained surface. The transformation is then used to map the coordinates of the DLPFC in the atlas to the subject’s space. Firstly, we found the surface sampling and reconstruction on the phantom to be accurate (mean error 1.6 mm, standard deviation 1.08 mm). Secondly, we compared the surface-based DLPFC localization to a ground truth localization performed by an expert in neuroanatomy. Results have shown on 10 subjects that the mean error was 10.2 mm.

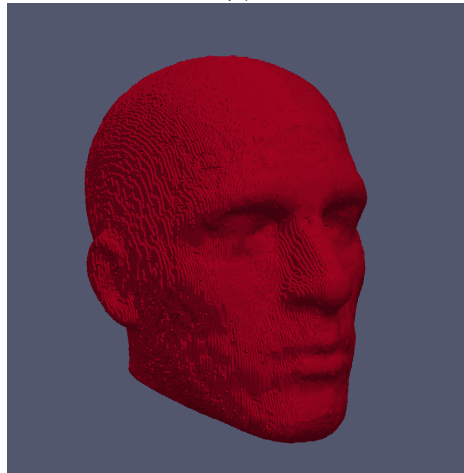
In a previous study [10], we have assessed the performance of 3 clinicians on 25 subjects to localize the DLPFC on MRI and found a large discrepancy between raters: accuracy compared to reference localization varied between 8 mm and 14 mm (standard deviation 5.7 mm). In comparison, the mean error of 10.2 mm can be considered acceptable. In addition, we focus on rTMS application where the electromagnetic field has some dispersion. Therefore, we argue that, although less accurate than neuronavigation using the subject’s MRI, this MRI-free neuronavigation technique is reproducible between sessions and is valuable for a routine clinical use of rTMS. Further work should 1) enlarge the database of subjects and extend this technique to other stimulation targets, such as the temporoparietal cortex to treat auditory hallucination in schizophrenia for instance and 2) evaluate the therapeutic efficiency on patients.



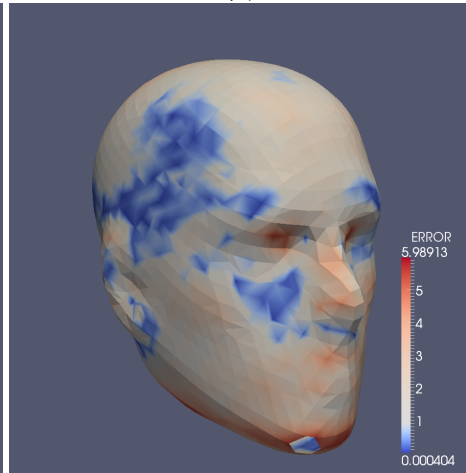
(a)



(b)



(c)



(d)

Fig. 2. This figure shows the validation of the acquisition and reconstruction of a point set on a physical-head phantom. (a) shows a picture of the physical phantom used to assess the surface acquisition and reconstruction method. (b) shows the acquired point set and the reconstructed Poisson surface. (c) shows the skin surface extracted from CT. (d) shows the Poisson surface registered to the CT surface. The color represents the spatial distribution of errors after reconstruction and registration. The mean point-to-point error was 1.6 mm with standard deviation was 1.08 mm.

	Landmark-based	Rigid	Affine	Non-linear
Subject 1	11.3	5.7	3.5	3.3
Subject 2	13.1	13.5	12.1	11.9
Subject 3	23.8	15.1	13.6	12.3
Subject 4	27.7	10.5	8.8	9.2
Subject 5	16.8	4.7	3.2	3.1
Subject 6	22.5	9.1	7.6	6.8
Subject 7	32.9	21	20.3	19.5
Subject 8	22.7	18.7	14.2	13.6
Subject 9	21.3	19.2	15.6	15.4
Subject 10	23.3	7.7	6.4	6.7
Mean (mm)	21.54	12.52	10.53	10.18
Std.dev. (mm)	6.46	5.86	5.56	5.33

Table 1. Results of the surface-based localization of the DLPFC when compared to the reference DLPFC. Various parametrization of the surface-based method were tested. The fully non-linear registration provided a mean error of 10.2 mm.

References

1. H. Chui, A. Rangarajan, Jie Zhang, and C. Morison Leonard. Unsupervised Learning of an Atlas from Unlabeled Point-Sets. *IEEE Transactions on Pattern Analysis and Machine Intelligence*, 26:160–172, 2004.
2. B. Combès and S. Prima. An Efficient EM-ICP Algorithm for Symmetric Consistent Non-linear Registration of Point Sets. In *MICCAI'2010*, volume 6362, pages 594–601. LNCS, 2010.
3. D. Doria and A. Gelas. Poisson surface reconstruction for VTK. *The VTK Journal*, 2010.
4. P.B. Fitzgerald, K. Hoy, S. McQueen, J.J. Maller, S. Herring, R. Segrave, M. Bailey, G. Been, J. Kulkarni, and Z.J. Daskalakis. A randomized trial of rTMS targeted with MRI based neuro-navigation in treatment-resistant depression. *Neuropsychopharmacology*, 34(5):1255–62, 2009.
5. S. Granger and X. Pennec. Multi-scale EM-ICP: A Fast and Robust Approach for Surface Registration. In *ECCV'2002*, volume 2353, pages 418–432. LNCS, 2002.
6. <http://www.cgal.org>. Computational Geometry Algorithms Library.
7. M. Kazhdan, M. Bolitho, and H. Hoppe. Poisson surface reconstruction. In *Eurographics Symposium on Geometry Processing*, 2006.
8. J. Koikkalainen, M. Könönen, J. Karhu, J. Ruohonen, E. Niskanen, and J. Lötjönen. Dynamic probabilistic atlas of functional brain regions for transcranial magnetic stimulation. In *MICCAI'2008*, volume 5241, pages 543–550. LNCS, 2008.
9. F. Lalys, C. Haegelen, J.-C. Ferré, O. El Ganaoui, and P. Jannin. Construction and assessment of a 3-T MRI brain template. *NeuroImage*, 49(1):345 – 354, 2010.
10. C. Nauczyciel, P. Hellier, B. Millet, and X. Morandi. Localization of the dorso-lateral prefrontal cortex in MRI images for neuronavigated TMS. *Submitted to Psychiatry research*.
11. C. Nauczyciel, P. Hellier, X. Morandi, S. Blestel, D. Drapier, J.-C. Ferré, C. Barillot, and B. Millet. Assessment of standard coil positioning in transcranial magnetic stimulation in depression. *Psychiatry research*, 186(2-3):232–238, 2011.

12. M. Petrides. Lateral prefrontal cortex: architectonic and functional organization. *Philos Trans R Soc Lond B Biol Sci*, 360(1456):781–795, 2005.
13. M. Ridding and J. Rothwell. Is there a future for therapeutic use of transcranial magnetic stimulation? *Nature Rev. Neurosci.*, 8:559–567, 2007.
14. H. Wendland. *Scattered Data Approximation*. Cambridge Monographs on Applied and Computational Mathematics, 2005.